Medicinal Chemistry Research (2019) 28:1633–1647
https://doi.org/10.1007/s00044-019-02400-x

MEDICINAL CHEMISTRY RESEARCH

ORIGINAL RESEARCH

Discovery of 3-(thiophen/thiazole-2-ylthio)pyridine derivatives as multitarget anticancer agents

Jiankang Zhang[1] · Jianjun Xi[2] · Ruoyu He[2] · Rangxiao Zhuang[2] · Limin Kong[3] · Liping Fu[4] · Yanmei Zhao[2] · Chong Zhang[1] · Linghui Zeng[1] · Jingyi Lu[1] · Rujia Tao[1] · Zhengmengtong Liu[1] · Huajian Zhu[1] · Shourong Liu[2]

Received: 26 April 2019 / Accepted: 16 July 2019 / Published online: 25 July 2019

Abstract

A series of novel 3-(thiophen/thiazole-2-ylthio)pyridine derivatives were designed and synthesized as IGF-1R tyrosine kinase inhibitors. All the target compounds were tested for their IGF-1R kinase inhibitory activities and cytotoxicities against five cancer cell lines (K562, Hep-G2, HCT-116, WSU-DLCL2, and A549). Although all these compounds exhibited moderate to potent cancer cell proliferation inhibitory activities (the most potent compound **43** showed IC_{50} value of 1.3 ± 0.9 μM against WSU-DLCL2 cell line), IGF-1R inhibition were not observed. In order to identify the exact target of these analogues, selected compounds were further screened for various kinases. The results indicated that this series of compounds may exert their anticancer activities through inhibiting various kinases including FGFR 3, EGFR, JAK, and RON. In addition, cell cycle analysis of compound **43** on Hep-G2 cells showed cell cycle arrest at G1/G0 phase. All the experiments validated the potential of 3-(thiophen/thiazole-2-ylthio)pyridine analogues as multi-target anticancer agents.

Keywords Multitarget · IGF-1R · Anti-cancer · Kinases

Introduction

The insulin-like growth factors (IGFs) belong to a multi-functional growth factor family, which plays a pivotal role in the regulation of normal physiological and pathological processes. The IGFs family consists of two ligands (IGF-1 and IGF-2), three cell-membrance receptors (IGF-1R, IGF-2R, and IR), and six IGF-binding proteins (IGFBP1-6) (Sun et al. 2017; Scagliotti and Novello 2012; Buchanan et al. 2011; Furstenberger and Senn 2002; Brahmkhatri et al. 2015). The IGF-1 is a single chain peptide, which is comprised of 70 amino acids in four domains (7.65 kDa). The IGF-1 binds to at least two cell surface receptor tyrosine kinases (RTKs): the IGF-1 receptor (IGF-1R) and the insulin receptor. The primary action of IGF-1 is mediated by binding to its specific receptor IGF-1R. The IGF-1R, a transmembrane receptor tyrosine kinase, is widely expressed in many cell types and tissues (LeRoith et al. 1995; Stewart and Rotwein 1996; Sepp-Lorenzino 1998). Through endocrine, paracrine, and autocrine mechanisms, IGF-1R exerts its mitogenic effect on various cells by stimulating proliferation and inhibiting apoptosis.

The tyrosine kinase activity was activated after binding of IGFs to IGF-1R, which leads to autophosphorylation. Furthermore, this phosphorylation results activation of various downstream signaling cascades. To date, two distinct IGF-IR signal transduction pathways have been identified: the mitogen activated protein kinase (RAS/RAF/MAPK) pathway that predominantly stimulates cellular proliferation, and the phosphatidylinositol-3-kinase-Akt pathway that chiefly mediates cell survival (Sachdev and Yee 2007; Samani et al. 2007; Kawauchi et al. 2009;

These authors contributed equally: Jiankang Zhang, Jianjun Xi

✉ Huajian Zhu
zhuhj@zucc.edu.cn

✉ Shourong Liu
liushourong85463990@sina.com

[1] School of Medicine, Zhejiang University City College, Hangzhou 310015 Zhejiang, China

[2] Department of Pharmaceutical Preparation, Hangzhou Xixi Hospital, Hangzhou 310023 Zhejiang, China

[3] Department of Pharmacy, The First Affiliated Hospital, College of Medicine, Zhejiang University, Hangzhou 310003 Zhejiang, China

[4] Department of Pharmacy, Shaoxing Hospital of Traditional Chinese Medicine, Shaoxing 312000 Zhejiang, China

Vanhaesebroeck and Alessi 2000). Due to its promotion roles in both processes, IGF-1R signaling is related to various physiological functions including differentiation, transformation, and prevention of apoptosis. In addition, studies indicated that IGF-1R overexpression is related to many human cancers, such as breast (Sun et al. 2015), prostate (Pollak et al. 1998), glioma (Trojan et al. 2007), and lung cancer (Yeo et al. 2015). Moreover, clinical studies also showed that high levels expression of IGF-1R in cancer was associated with tumor metastasis, resistance, poor prognosis, and shortened survival (Sun et al. 2017). Therefore, IGF-1R has become a potential and promising diagnostic and therapeutic target in cancers.

To date, more than two dozen of antagonistic monoclonal antibodies and small molecule inhibitors against IGF-1R have been developed. Currently, at least 12 randomized controlled clinical trials are ongoing (NCT00887159, NCT00799240) (Gualberto and Pollak 2009; Rodon et al. 2008). Linsitinib (OSI-906) (Mulvihill et al. 2009), a Phase III clinical candidate, has been evaluated for metastatic adrenocortical carcinoma, and is also studied in combination with other anticancer agents. BMS-754807 (Carboni et al. 2009) was developed by Bristol-Myers Squibb in a Phase II clinical trial for breast cancer. Picropodephyllin (Girnita et al. 2004) is currently in Phase II/III for the treatment of a variety of cancers, while Nordihydroguaiaretic acid (Hewish et al. 2009) is in a Phase II clinical trial and evaluated for prostate cancer (Fig. 1).

III-**106** (Fig. 2), an ATP competitive IGF-1R inhibitor with a new aminopyrazoloquinazolines scaffold, was discovered by Boehringer Ingelheim International GmbH with 50% inhibitory concentration (IC_{50}) value of 5 nM (Treu 2010). However, the poor selectivity and severe side effects of the majority of the ATP competitive inhibitors limited its further application (Deng et al. 2007). In order to reduce toxicities while retain IGF-1R inhibitory activities, a novel series of 3-(thiophen/thiazole -2-ylthio)pyridine analogues were designed and synthesized with III-**106** employed as the lead compound.

In this study, 3D similarity analysis and docking studies were performed to verify the design strategy. The 3D shape similarity comparison is an important strategy for evaluating whether designed analogues were consistent with the lead compound. Compounds with high structural similarity could generate similar activity. The active compound should have suitable shape to fit the target pocket. Therefore, 3D similarity is a potential method to find active compounds. The designed compounds **34**, **35**, **43**, **44**, **47**, and **50** were selected in comparison with III-**106** for their 3D similarity, and the similarity score of each comparison were calculated. As shown in Table 1, compound **43** exhibited a higher similarity score of 0.67 compared with III-**106**. Afterwards, the binding modes of compounds were predicted by computational methods. Compound **43** was prepared and docked into the active site of IGF-1R (PDB code: 5FXS) using Glide under default setting. As shown in Fig. 3, the pyridine core formed a hydrogen bond with the N-H of Met84 in the hinge region, and the isopropyl benzene ring extended into the P-loop region. In addition, the thiophene ring was located into the channel to the solvent region, while the nitro group formed a hydrogen bond with the Arg5 of P-loop. All these hydrogen bonds formed play an important role in the activity of the compound. These results verify the reliability of the design strategy, and target compound synthesis and evaluation were performed in this study.

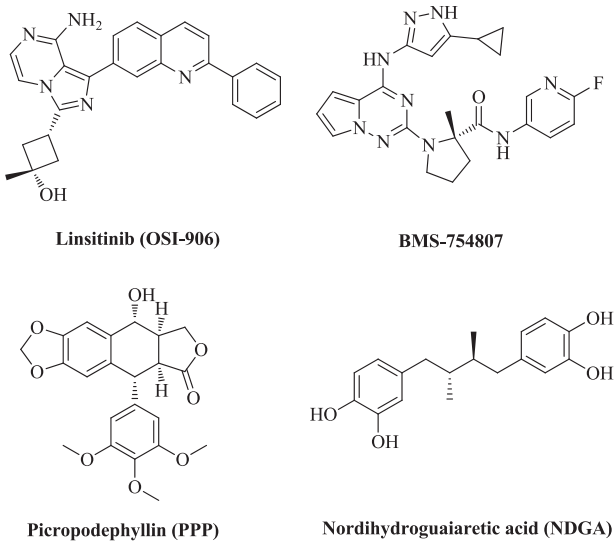

Fig. 1 Small-molecule IGF-1R inhibitors in clinical trials

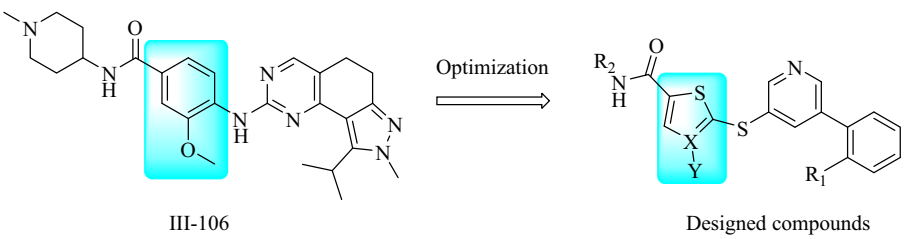

Fig. 2 Design strategy of the new synthesized IGF-1R inhibitors

Results and discussion

Chemistry

The synthetic route for intermediates **3**, **5**, and **7** were prepared as outlined in Scheme 1. Fragments **2** and **5** were synthesized by esterification of the corresponding acids **1** and **4** with methanol in the presence of catalytic amount of hydrochloric acid. Afterwards, the synthesized ester **2** was converted to fragment **5** by nitration reaction in a mixture solution of HNO_3 in H_2SO_4. Fragment **7** can be easily obtained from methyl 4-cyano-5-(methylthio)thiophene-2-carboxylate (**6**) with m-CPBA. And fragment **9** was synthesized by 3, 5-dibromopyridine (**8**) and 4-methoxy-α-toluenethiol under alkaline conditions. The target compounds **31–50** were synthesized following the route described in Scheme 2. Firstly, intermediates **11a–c** were prepared by coupling from fragment **9** with different boric acids, and cleavage of the thioether bound provided **12a–c**. Subsequently, **12a–c** coupled with fragments **3**, **5** and **7** to afford **13–18**, then hydrolyzed to give **19–24**, which was transformed to the acyl chloride at the presence of $(COCl)_2$. Finally, acyl chloride reacted with different aryl amine to afford the target compounds **31–50**.

Table 1 The similarity scores of target compounds

Compound	Similarity score
34	0.37
35	0.56
43	**0.67**
44	0.51
47	0.52
50	0.42

IGF-1R inhibitory activities

All the target compounds (**31–50**) were screened for their IGF-1R inhibitory activities in vitro by electrophoretic mobility shift assay using Staurosporine as positive control. The results showed that all the compounds exerted no inhibitory activities against IGF-1R kinase with IC_{50} values >30 μM. In view of this, all the target compounds were tested for antitumor activities against different cell lines.

Cell proliferation assay

All the target compounds (**31–50**) were further screened for their antiproliferative activities in vitro against five cancer cell lines (K562, Hep-G2, HCT-116, WSU-DLCL2, and A549) through standard CTG assay (Paclitaxel as positive control). As illustrated in Table 2, all the compounds displayed various degrees of cytotoxic activities against five cancer cell lines. Among all of these compounds, **43** and **44** showed excellent inhibitory activities against WSU-DLCL2 cell line with IC_{50} values of 1.3 ± 0.9 and 1.3 ± 1.8 μM, respectively.

In vitro kinase screening

Subsequently, compound **43** was further screened for about 41 kinases inhibitory profiles on the DiscoverX's KinomeScan profiling platform. Measurements were performed at a concentration of 10 μM, and the results were illustrated in Table 3. We defined the kinases results for primary screen

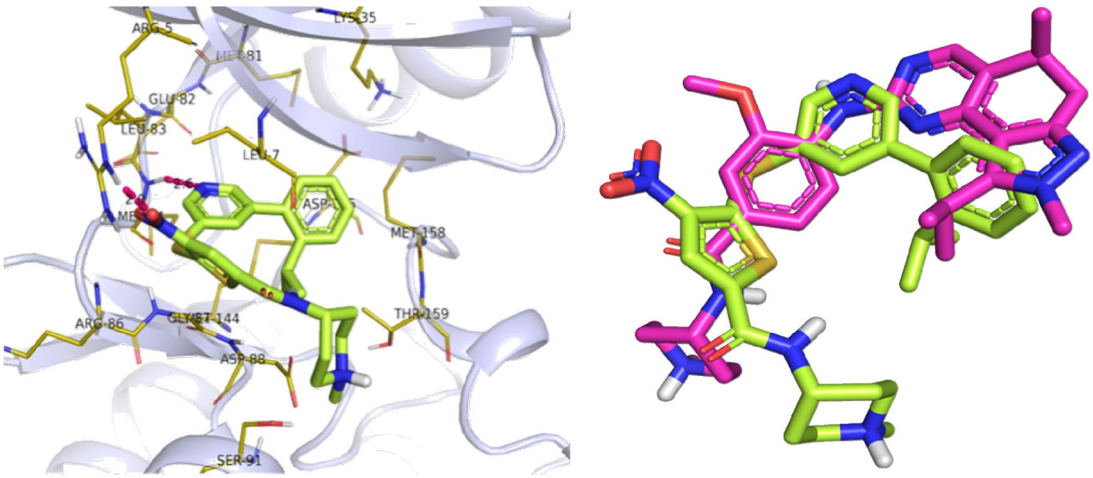

(A) (B)

Fig. 3 **a** The binding mode of selected compound **43** with IGF-1R (PDB code: 5FSX). **b** Superposition of compound **43** (green) and compound **III-106** (pink)

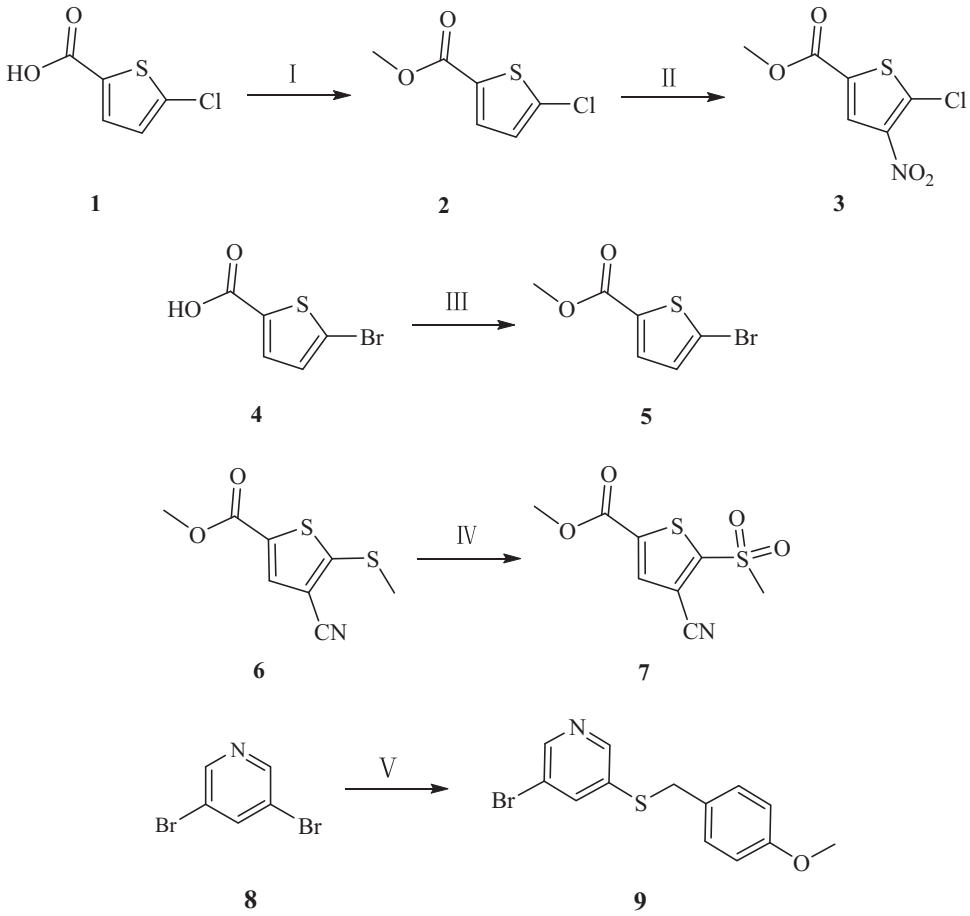

Scheme 1 Reagents and conditions: (I) HCl/MeOH, 60 °C, 16 h; (II) H_2SO_4/HNO_3, 0 °C, 3 h; (III) HCl/MeOH, 60 °C, 16 h; (IV) *m*-CPBA, DCM, 25 °C, 16 h. (V) 4-Methoxy-α-toluenethiol, NaH, DMF, 20 °C, 16 h

binding interactions reported as percent control (% Ctrl). The % Ctrl indicated that the dissociative kinases (unbound to **43**) were the percentages of all tested kinases, where lower numbers indicated stronger binding to **43**. The obtained data demonstrated that compound **43** has weakly or no % Ctrl against 41 kinases tested. Compound **43** showed weak % Ctrl against other kinases, such as HPKE (84%), ERK3 (86%), ERK4 (87%), MAK (79%), and MINK (86%). In addition, the % Ctrl of **43** against AUR A, JAK3, FGFR2, FGFR3, EGFR, and RON were tested with threefold serial dilutions starting at concentration of 30 μM, and the results were summarized in Table 4. Inspiringly, compound **43** showed good inhibitory activities against these kinases with IC_{50} values ranging from 2 to 22 μM (except AUR A), and especially with an IC_{50} value of 2.0 ± 0.3 μM against FGFR3.

Cell cycle analysis

The effect of compound **43** on Hep-G2 cell cycle was studied by flow cytometric analysis. Hep-G2 cell was treated with compound **43** (0.5, 1, 5, and 10 μM) or Doxorubicin (0.5 and 1 μM) for 24 h. Results showed that there was a significant alterations in cell cycle phases (Fig. 2). Treatment with compound **43** (0.5, 5, and 10 μM, respectively) caused an increase in the percentage of apoptotic cells at G1/G0 phase (72.18%, 75.09% and 74.86%, respectively) compared with control (67.08%). The percentage of cells at S phase (21.05%, 17.80% and 17.91%, respectively) has a concurrent reduction compared with control (25.04%), and no significant difference was found in the percent of cells at the G2/M phase. By contrast, there was a significant decrease in the cells at G1/G0 phase (50.01% and 46.75%) of Doxorubicin (0.5 and 1 μM) compared with control, and the percentage of cells at the G2/M phase increased from 7.88% to 27.30% and 16.93%, respectively. The result indicated that compound **43** induces cell cycle arrest at the G1/G0 phase on Hep-G2 cells, while Doxorubicin showed a significant arrest at the G2/M phase (Fig. 4).

Experimental procedures

Chemistry

The ^{1}H and ^{13}C NMR spectra were recorded on Brüker 400 MHz spectrometer (Brüker Bioscience, Billerica, MA,

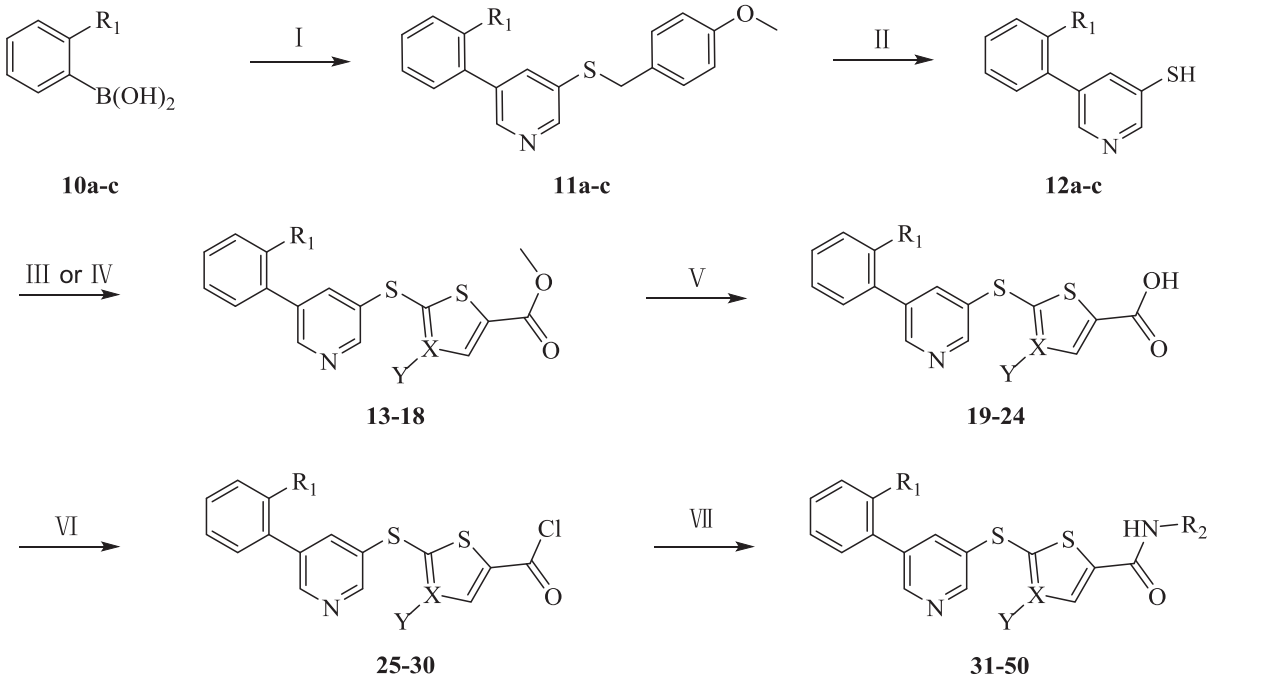

a, R_1 = isopropyl; **b**, R_1 = ethyl; **c**, R_1 = methoxy

13, **19**, **25**, R_1 = isopropyl; X = N; **14**, **20**, **26**, R_1 = methoxy; X = N; **15**, **21**, **27**, R_1 = ethyl; X = N;

16, **22**, **28**, R_1 = isopropyl; X = C; Y = NO_2; **17**, **23**, **29**, R_1 = isopropyl; X = C; Y = CN; **18**, **24**, **30**, R_1 = isopropyl; X = C; Y = H;

	R_1	R_2	X	Y
31	isopropyl	phenyl	N	-
32	isopropyl	4-fluorophenyl	N	-
33	isopropyl	4-methoxyphenyl	N	-
34	isopropyl	benzyl	N	-
35	isopropyl	1-methyl-4-piperidyl	N	-
36	isopropyl	4-methyl-1-piperazy	N	-
37	ethyl	4-fluorophenyl	N	-
38	ethyl	benzyl	N	-
39	4-methoxyphenyl	4-fluorophenyl	N	-
40	4-methoxyphenyl	benzyl	N	-
41	isopropyl	4-fluorophenyl	C	NO_2
42	isopropyl	benzyl	C	NO_2
43	isopropyl	1-methyl-4-piperidyl	C	NO_2
44	isopropyl	4-methyl-1-piperazyl	C	NO_2
45	isopropyl	4-fluorophenyl	C	CN
46	isopropyl	benzyl	C	CN
47	isopropyl	1-methyl-4-piperidyl	C	CN
48	isopropyl	4-methyl-1-piperazy	C	CN
49	isopropyl	4-fluorophenyl	C	H
50	isopropyl	benzyl	C	H

Scheme 2 Reagents and conditions: (I) Pd(dppf)Cl_2, Na_2CO_3, Dioxane/H_2O, 100 °C, 16 h; (II) $AlCl_3$, toluene, 25 °C, 3 h; (III) K_2CO_3, CH_3CN, 82 °C, 16 h; (IV) CuI, K_2CO_3, DMSO, 80 °C, 16 h; (V) NaOH, MeOH/H_2O, 25 °C, 2 h; (VI) DMF, $(COCl)_2$, DCM, 25 °C, 1 h; (VII) Et_3N, DCM, 25 °C, 16 h

USA) with $CDCl_3$ or d_6-DMSO as solvent. Chemical shifts (δ) were reported in parts per million relative to internal TMS, and coupling constants (J) were reported in Hertz (Hz). Splitting patterns were designated as singlet (s), broad singlet (brs), doublet (d), double doublet (dd), triplet (t), quartet (q), and multiplet (m). Mass spectral data were obtained by Esquire-LC-00075 spectrometer (Brüker Bioscience). Reagents and solvents were purchased from common commercial suppliers and were used without further purification unless stated otherwise. Column chromatography was performed using silica gel (300–400 mesh). All yields are unoptimized and generally represent the result of a single experiment.

Synthesis of methyl 5-chlorothiophene-2-carboxylate (2)

A solution of 5-chloro-2-thiophenecarboxylic acid (**1**, 90.0 g, 553.5 mmol, 1.0 eq) in HCl/MeOH (500.0 mL) was

Table 2 In vitro antiproliferative activities of the target compounds against various cancer cell lines

Compound	IC_{50}[a], (μM)				
	K562	Hep-G2	HCT-116	WSU-DLCL2	A549
31	40.1 ± 3.3	23.4 ± 1.2	34.7 ± 5.4	28.3 ± 2.9	38.9 ± 7.8
32	24.8 ± 1.8	16.9 ± 2.6	23.8 ± 2.8	27.4 ± 1.7	31.6 ± 3.5
33	3.7 ± 0.9	NA[b]	2.9 ± 0.6	3.8 ± 0.4	3.2 ± 1.5
34	18.2 ± 1.7	12.3 ± 2.2	10.6 ± 1.1	18.1 ± 1.2	16.7 ± 0.7
35	5.2 ± 0.5	5.6 ± 0.1	7.4 ± 2.0	12.3 ± 3.4	34.8 ± 8.6
36	29.0 ± 4.9	25.8 ± 8.4	26.2 ± 2.4	35.4 ± 8.1	61.1 ± 16.3
37	32.9 ± 8.7	22.7 ± 5.5	27.3 ± 1.8	29.7 ± 3.6	39.7 ± 10.8
38	38.7 ± 5.3	21.6 ± 6.1	32.4 ± 6.4	32.5 ± 6.4	37.2 ± 6.5
39	38.2 ± 3.4	20.0 ± 1.3	28.9 ± 1.9	33.7 ± 0.9	57.5 ± 9.9
40	27.2 ± 2.9	56.1 ± 12.1	75.8 ± 15.7	40.9 ± 10.5	66.8 ± 2.6
41	11.7 ± 3.1	13.9 ± 3.0	7.6 ± 0.9	3.0 ± 1.1	35.1 ± 13.3
42	12.9 ± 1.1	6.8 ± 1.6	8.4 ± 1.5	6.0 ± 2.6	30.9 ± 6.6
43	5.1 ± 2.5	5.1 ± 0.3	13.2 ± 1.1	1.3 ± 0.9	28.1 ± 5.3
44	5.5 ± 0.6	9.9 ± 1.9	7.6 ± 2.5	1.3 ± 1.8	25.2 ± 2.7
45	9.8 ± 1.7	4.8 ± 2.4	7.6 ± 1.3	5.6 ± 3.1	10.9 ± 3.6
46	12.2 ± 2.8	13.3 ± 1.0	5.5 ± 2.2	13.4 ± 2.2	11.6 ± 1.1
47	6.4 ± 1.4	5.1 ± 0.7	6.1 ± 1.0	9.9 ± 1.7	18.9 ± 0.8
48	26.9 ± 6.9	23.8 ± 2.5	25.6 ± 6.5	22.7 ± 4.3	33.8 ± 9.1
49	16.9 ± 1.1	13.9 ± 3.3	10.6 ± 1.8	23.5 ± 6.1	27.6 ± 2.6
50	11.2 ± 0.5	11.7 ± 2.9	8.8 ± 1.6	14.9 ± 1.0	13.9 ± 2.9
Paclitaxel[c](nM)	3.4 ± 0.3	10.2 ± 3.8	1.2 ± 0.2	2.1 ± 0.2	2.0 ± 0.3

[a]The values are an average of three separate determinations

[b]Not active in the highest concentration used

[c]Used as positive control

stirred at 60 °C for 16 h. The reaction mixture was then concentrated in vacuo. The residue was dissolved in EtOAc (500.0 mL), washed with $NaHCO_3$ (aq.) to pH = 8–9. The organic layer was dried over Na_2SO_4 and concentrated in vacuo to give compound **2**. Yellow oil; Yield: 94.1%; ^{1}H NMR (400 MHz, $CDCl_3$): $\delta = 7.58$ (d, $J = 4.0$ Hz, 1H, thienyl-H), 6.93 (d, $J = 4.0$ Hz, 1H, thienyl-H), and 3.87 (s, 3H, CH_3). ESI-MS: m/z = 178.0$[M + H]^+$.

Synthesis of methyl 5-chloro-4-nitrothiophene-2-carboxylate (3)

To a solution of compound **2** (30.0 g, 169.9 mmol, 1.0 eq) in con.H_2SO_4 (60.0 mL) was added a mixture of con.HNO_3 (12.8 g, 203.8 mmol, 9.2 mL, 1.2 eq) in con.H_2SO_4 (12.0 mL). The reaction was stirred at 0 °C for 3 h. The reaction was quenched with ice-water (100.0 mL), extracted with EtOAc (100.0 mL × 3). The combined organic layer was dried over Na_2SO_4 and concentrated under reduced pressure. The crude product was purified by CombiFlash (0–10% EtOAc in PE) to give compound **3** as white solid. Yield: 47.8%; ^{1}H NMR (400 MHz, $CDCl_3$) : $\delta = 8.19$ (s, 1H, thienyl-H), and 3.94 (s, 3H, CH_3). ESI-MS: m/z = 222.9$[M + H]^+$.

Synthesis of methyl 5-bromothiophene-2-carboxylate (5)

A solution of 5-bromo-2-thiophenecarboxylic acid (**4**, 90.0 g, 553.5 mmol, 1.0 eq) in HCl/MeOH (500.0 mL) was stirred at 60 °C for 16 h. The reaction was concentrated in vacuo. The residue was dissolved in EtOAc (500.0 mL) and washed with $NaHCO_3$(aq.) to pH = 8–9, then the organic layer was dried over Na_2SO_4 and concentrated in vacuo to give compound **5**. Yellow oil; Yield: 94.1%; ^{1}H NMR (400 MHz, $CDCl_3$): $\delta = 7.55$ (d, $J = 4.0$ Hz, 1H, thienyl-H), 7.07 (d, $J = 4.0$ Hz, 1H, thienyl-H), and 3.87 (s, 3H, CH_3). ESI-MS: m/z = 222.3$[M + H]^+$.

Synthesis of methyl 4-cyano-5-(methylsulfonyl)thiophene-2-carboxylate (7)

To a solution of methyl 4-cyano-5-(methylthio)thiophene-2-carboxylate (**6**, 550.0 mg, 2.6 mmol, 1.0 eq) in CH_2Cl_2 (10.0 mL) was added *m*-CPBA (1.3 g, 6.5 mmol, 85.0% purity, 2.5 eq). The reaction was stirred at 25 °C for 16 h. The reaction was quenched with Na_2SO_3 (aq., 200.00 mL), and extracted with CH_2Cl_2 (20.0 mL × 3). The combined organic layer was washed with 1N NaOH (200.0 mL), dried

Table 3 Results of compound **43** against about 50 kinases

Target/Gene symbol	% Ctrl[a]	Target/Gene symbol	% Ctrl[a]
AKT1	97	FGFR4	100
AKT2	100	HCK	100
AKT3	100	HPK1	84
AURKB	100	INSR	98
AURKC	97	SRC	95
BTK	100	TEC	100
DAPK1	96	VEGFR2	100
DAPK2	100	KIT	94
DAPK3	95	MAK	79
DDR1	96	MAP3K1	100
DDR2	100	MARK1	97
DMPK	100	MARK2	100
ERK1	100	MINK	86
ERK2	96	PAK7	100
ERK3	86	PCTK3	93
ERK4	87	PDPK1	100
ERK5	94	QSK	100
ERK8	100	RAF1	100
FAK	100	ROCK1	100
FGFR1	100	ROCK2	100
SLK	95		

[a]% Ctrl was measured by method (A) at a concentration of 10 μM

Table 4 Kinase inhibitory assay of compound **43**

Kinase	IC_{50}[a], (μM)
FGFR2	22.6 ± 2.9
FGFR3	2.0 ± 0.3
EGFR	8.9 ± 3.4
JAK3	12.4 ± 2.1
RON	11.6 ± 1.0
AUR A	> 30

[a]The values are an average of three separate determinations, measured through method (B)

over Na_2SO_4 and concentrated under reduced pressure to give compound **7**. White solid; Yield: 93.2%; ^{1}H NMR (400 MHz, $CDCl_3$): $\delta = 7.92$ (s, 1H, thienyl-H), 3.91 (s, 3H, CH_3), and 3.30 (s, 3H, CH_3). ESI-MS: m/z = 245.7 $[M + H]^+$.

Synthesis of 3-bromo-5-((4-methoxybenzyl)thio)pyridine (9)

To a solution of 4-methoxy-α-toluenethiol (32.6 g, 211.1 mmol, 29.3 mL, 1.0 eq) in DMF (500.0 mL) was added NaH (9.3 g, 232.2 mmol, 60.0% purity, 1.1 eq) at 20 °C, after stirring 30 min, 3,5-dibromopyridine (**8**, 50.0 g, 211.1 mmol, 1.0 eq) was added. The reaction was stirred at 20 °C for 16 h. The reaction was quenched with water (100.0 mL), extracted with EtOAc (100.0 mL × 3). The combined organic layer was washed with water (200.0 mL × 3), dried over Na_2SO_4 and concentrated in vacuo. The crude product was purified by CombiFlash (10% EtOAc in PE) to give the compound **9**. White solid; Yield: 73.0%; ^{1}H NMR (400 MHz, $CDCl_3$): $\delta = 8.38$ (d, $J = 2.0$ Hz, 1H, pyridine-H), 8.31 (d, $J = 2.0$ Hz, 1H, pyridine-H), 7.60 (t, $J = 2.0$ Hz, 1H, pyridine-H), 7.13–7.08 (m, 2H, Ar-H), 6.79–6.73 (m, 2H, Ar-H), 4.00 (s, 2H, CH_2), and 3.71 (s, 3H, CH_3). ESI-MS: m/z = 311.7$[M + H]^+$.

General procedure for the synthesis of compounds 11a–c

A mixture of compounds **10a–c** (53.2 mmol, 1.1 eq), compound **9** (15.0 g, 48.4 mmol, 1.0 eq), Pd(dppf)Cl_2 (3.5 g, 4.8 mmol, 0.1 eq), and Na_2CO_3 (10.2 g, 96.7 mmol, 2.0 eq) in dioxane/H_2O (10/1, 150.0 mL) was stirred at 100 °C for 16 h. The mixture was concentrated in vacuo, diluted with water (20.0 mL), and extracted with CH_2Cl_2 (50.0 mL × 3). The combined organic layer was dried over Na_2SO_4 and concentrated under reduced pressure. The crude product was purified by CombiFlash (20% EtOAc in PE) to give the compounds **11a–c**.

3-(2-isopropylphenyl)-5-((4-methoxybenzyl)thio)pyridine (11a) Yellow oil; Yield: 78.1%; ^{1}H NMR (400 MHz, $CDCl_3$): $\delta = 8.52$ (d, $J = 2.4$ Hz, 1H, pyridine-H), 8.36 (d, $J = 2.0$ Hz, 1H, pyridine-H), 7.48 (t, $J = 2.0$ Hz, 1H, pyridine-H), 7.41–7.38 (m, 2H, Ar-H), 7.24–7.17 (m, 3H, Ar-H), 7.07 (d, $J = 7.2$ Hz, 1H, Ar-H), 6.81 (d, $J = 8.4$ Hz, 2H, Ar-H), 4.10 (s, 2H, CH_2), 3.78 (s, 3H, CH_3), 2.90–2.83 (m, 1H, CH), and 1.14 (d, $J = 6.4$ Hz, 6H, $2CH_3$). ESI-MS: m/z = 350.9$[M + H]^+$.

3-(2-ethylphenyl)-5-((4-methoxybenzyl)thio)pyridine (11b) Yellow oil; Yield: 72.1%; ^{1}H NMR (400 MHz, $CDCl_3$): $\delta = 8.52$ (d, $J = 2.0$ Hz, 1H, pyridine-H), 8.38 (d, $J = 2.0$ Hz, 1H, pyridine-H), 7.50 (t, $J = 2.0$ Hz, 1H, pyridine-H), 7.37–7.17 (m, 5H, Ar-H), 7.10 (d, $J = 7.6$ Hz, 1H, Ar-H), 6.81 (d, $J = 8.8$ Hz, 2H, Ar-H), 4.10 (s, 2H, CH_2), 3.78 (s, 3H, CH_3), 2.50 (q, $J = 7.6$, 15.2 Hz, 2H, CH_2), and 1.07 (t, $J = 7.5$ Hz, 3H, CH_3). ESI-MS: m/z = 336.1$[M + H]^+$.

3-((4-methoxybenzyl)thio)-5-(2-methoxyphenyl)pyridine (11c) Yellow oil; Yield: 64.5%; ^{1}H NMR (400 MHz, $CDCl_3$): $\delta = 8.58$ (d, $J = 2.0$ Hz, 1H, pyridine-H), 8.46 (d, $J = 2.0$ Hz, 1H, pyridine-H), 7.75 (t, $J = 2.0$ Hz, 1H, pyridine-H), 7.39–7.35 (m, 1H, Ar-H), 7.26–7.19 (m, 3H, Ar-H), 7.06–6.98 (m, 2H, Ar-H), 6.84–6.82 (m, 2H, Ar-H), 4.11 (s, 2H, CH_2), 3.81 (s, 3H,CH_3), and 3.78 (s, 3H, CH_3). ESI-MS: m/z = 338.2$[M + H]^+$.

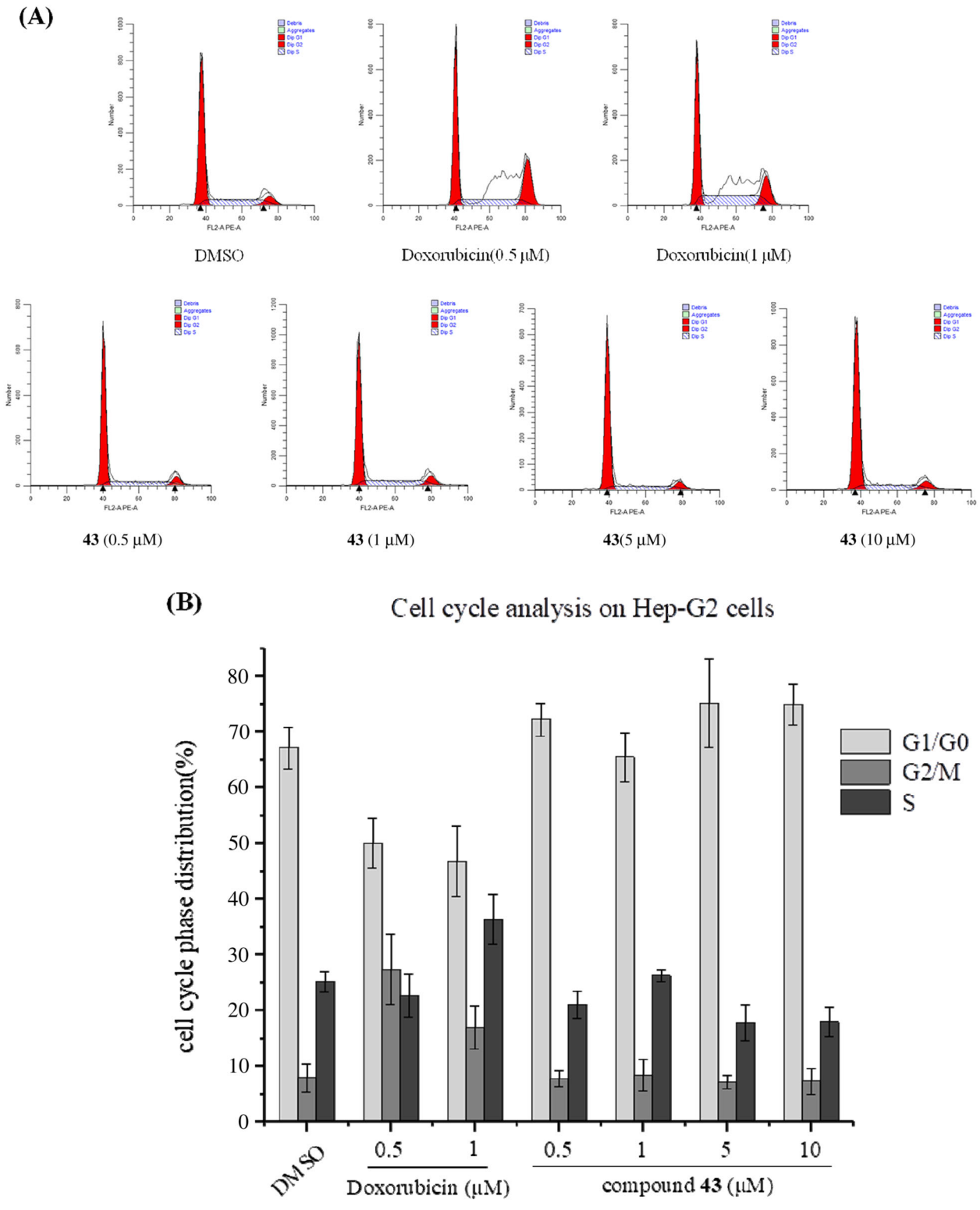

Fig. 4 Effect of compound **43** and Doxorubicin on flow cytometric analysis of Hep-G2 cells (**a**, **b**). The cells treated with DMSO were used as control

General procedure for the synthesis of compounds 12a–c

To a mixture of $AlCl_3$ (6.9 g, 51.5 mmol, 2.8 mL, 3.0 eq) in toluene (50.0 mL) was added a solution of compounds **11a–c** (17.2 mmol, 1.0 eq) in toluene (50.0 mL). The reaction was stirred at 25 °C for 3 h. The reaction was quenched with water (500.0 mL), extracted with EtOAc (500.0 mL × 3). The combined organic layer was dried over Na_2SO_4 and concentrated in vacuo. The residue was diluted with EtOAc (500.0 mL), washed with Na_2CO_3 (aq., 200.0 mL × 3). Then the water layer was acidified to pH = 2–3 with 1N HCl. The mixture was extracted with EtOAc (100.0 mL × 3), the combined organic layer was dried over Na_2SO_4 and concentrated under reduced pressure to give the compounds **12a–c**.

5-(2-isopropylphenyl)pyridine-3-thiol (12a) Yellow oil; Yield: 70.9%; ^{1}H NMR (400 MHz, $CDCl_3$): $\delta = 8.44$ (d, $J = 2.0$ Hz, 1H, pyridine-H), 8.28 (d, $J = 2.0$ Hz, 1H, pyridine-H), 7.48 (t, $J = 2.0$ Hz, 1H, pyridine-H), 7.34–7.30 (m, 2H, Ar-H), 7.19–7.15 (m, 1H, Ar-H), 7.07–7.05 (m, 1H, Ar-H), 2.92–2.82 (m, 1H, CH), and 1.10 (d, $J = 6.8$ Hz, 6H, $2CH_3$). ESI-MS: m/z = 230.1$[M + H]^+$.

5-(2-ethylphenyl)pyridine-3-thiol (12b) Yellow oil; Yield: 91.9%; ^{1}H NMR (400 MHz, $CDCl_3$): $\delta = 8.43$ (d, $J =$ 2.0 Hz, 1H, pyridine-H), 8.30 (d, $J = 2.0$ Hz, 1H, pyridine-H), 7.50 (t, $J = 2.0$ Hz, 1H, pyridine-H), 7.31–7.25 (m, 2H, Ar-H), 7.21–7.17 (m, 1H, Ar-H), 7.09–7.01 (m, 1H, Ar-H), 2.50 (q, $J = 7.6$, 14.8 Hz, 2H, CH_2), and 1.04 (t, $J = 7.6$ Hz, 3H, CH_3). ESI-MS: m/z = 216.1$[M + H]^+$.

5-(2-methoxyphenyl)pyridine-3-thiol (12c) Yellow oil; Yield: 48.3%; ^{1}H NMR (400 MHz, $CDCl_3$): $\delta = 8.48$ (d, $J = 2.0$ Hz, 1H, pyridine-H), 8.38 (d, $J = 2.0$ Hz, 1H, pyridine-H), 7.72 (t, $J = 2.0$ Hz, 1H, pyridine-H), 7.33–7.28 (m, 1H, Ar-H), 7.23–7.19 (m, 1H, Ar-H), 7.01–6.92 (m, 2H, Ar-H), and 3.75 (s, 3H, CH_3). ESI-MS: m/z = 218.1$[M + H]^+$.

General procedure for the synthesis of compounds 13–15

A mixture of compounds **12a–c** (6.5 mmol, 1.0 eq), methyl 2-chlorothiazole-5-carboxylate (1.2 g, 6.5 mmol, 1.0 eq), and K_2CO_3 (904.0 mg, 6.5 mmol, 1.0 eq) in CH_3CN (10.0 mL) was stirred at 82 °C for 16 h. The mixture was concentrated to give the crude compounds **13**–**15**, which was put into next step without further purification.

General procedure for the synthesis of compounds 16–17

A mixture of compound **12a** (699.5 mg, 3.0 mmol, 1.0 eq), compound **3** or **7** (3.0 mmol, 1.0 eq), and K_2CO_3 (843.1 mg, 6.1 mmol, 2.0 eq) in CH_3CN (10.0 mL) was stirred at 100 °C for 2 h (for compound **17**, stirring 16 h at 82 °C). The mixture was concentrated in vacuo to give the crude product **16** or **17**, which was put into next step without further purification.

Methyl 5-((5-(2-isopropylphenyl)pyridin-3-yl)thio)-4-nitrothiophene-2-carboxylate (18)

A mixture of compound **12a** (750.0 mg, 3.3 mmol, 1.0 eq), compound **5** (723.0 mg, 3.3 mmol, 1.0 eq), CuI (62.3 mg, 327.0 μmol, 0.1 eq), and K_2CO_3 (904.0 mg, 6.5 mmol, 2.0 eq) in DMSO (5.0 mL) was stirred at 80 °C for 16 h. The reaction was quenched with water (50.0 mL), and the mixture was acidified to pH = 2–3 with 1N HCl, extracted with EtOAc (100.0 mL × 3). The combined organic layer was dried over Na_2SO_4 and concentrated under reduced pressure to give the crude compound **18**, which was put into next step without further purification.

General procedure for the synthesis of compounds 19–24

A solution of compounds **13**–**18** (1.6 mmol, 1.0 eq) and NaOH (129.6 mg, 3.2 mmol, 2.0 eq) in MeOH/H_2O (10/1, 10.0 mL) was stirred at 25 °C for 2 h. The mixture was concentrated in vacuo. The residue was diluted with water, extracted with methyl tert-butyl ether (50.0 mL × 2). Then the pH of the water layer was adjusted to pH = 2 with 1N HCl, the mixture was extracted with EtOAc (100.0 mL × 3). The combined organic layer was dried over Na_2SO_4 and concentrated to give the compounds **19**–**24**.

2-((5-(2-isopropylphenyl)pyridin-3-yl)thio)thiazole-5-carboxylic acid (19) ^{1}H NMR (400 MHz, d_6-DMSO): $\delta =$ 8.95 (d, $J = 2.0$ Hz, 1H, pyridine-H), 8.75 (d, $J = 2.0$ Hz, 1H, pyridine-H), 8.29 (s, 1H, thiazole-H), 8.23 (t, $J =$ 2.0 Hz, 1H, pyridine-H), 7.55–7.46 (m, 2H, Ar-H), 7.38–7.34 (m, 1H, Ar-H), 7.30–7.28 (m, 1H, Ar-H), 3.00–2.93 (m, 1H, CH), and 1.18 (d, $J = 6.8$ Hz, 6H, $2CH_3$). ESI-MS: m/z = 357.1$[M + H]^+$.

2-((5-(2-methoxyphenyl)pyridin-3-yl)thio)thiazole-5-carboxylic acid (20) ^{1}H NMR (400 MHz, d_6-DMSO): $\delta =$ 8.86 (d, $J = 2.0$ Hz, 1H, pyridine-H), 8.82 (d, $J = 2.0$ Hz, 1H, pyridine-H), 8.33 (t, $J = 2.4$ Hz, 1H, thiazole-H), 8.25 (s, 1H, pyridine-H), 7.47–7.43 (m, 2H, Ar-H), 7.19–7.17 (m, 1H, Ar-H), 7.11–7.07 (m, 1H, Ar-H), and 3.80 (s, 3H, CH_3). ESI-MS: m/z = 345.0$[M + H]^+$.

2-((5-(2-ethylphenyl)pyridin-3-yl)thio)thiazole-5-carboxylic acid (21) ^{1}H NMR (400 MHz, d_6-DMSO): $\delta = 8.89$ (d, $J = 2.0$ Hz, 1H, pyridine-H), 8.72 (d, $J = 2.0$ Hz, 1H, pyridine-H), 8.24 (s, 1H, thiazole-H), 8.23 (t, $J = 2.0$ Hz, 1H, pyridine-H), 7.43–7.38 (m, 2H, Ar-H), 7.34–7.30 (m, 1H, Ar-H), 7.28–7.26 (m, 1H, Ar-H), 2.58 (q, $J = 7.6$, 15.2 Hz,

2H, CH), and 1.02 (t, $J = 3.6$ Hz, 3H, CH_3). ESI-MS: m/z = 343.1$[M + H]^+$.

5-((5-(2-isopropylphenyl)pyridin-3-yl)thio)-4-nitrothiophene-2-carboxylic acid (22) ^{1}H NMR (400 MHz, d_6-DMSO): $\delta = 8.94$ (d, $J = 2.0$ Hz, 1H, pyridine-H), 8.78 (d, $J = 2.0$ Hz, 1H, pyridine-H), 8.28 (t, $J = 2.4$ Hz, 1H, pyridine-H), 8.07 (s, 1H, thienyl-H), 7.50–7.43 (m, 2H, Ar-H), 7.31–7.24 (m, 2H, Ar-H), 2.97–2.91 (m, 1H, CH), 1.13 (d, $J = 6.8$ Hz, 6H, $2CH_3$). ESI-MS: m/z = 400.8$[M + H]^+$.

4-cyano-5-((5-(2-isopropylphenyl)pyridin-3-yl)thio)thiophene-2-carboxylic acid (23) ^{1}H NMR (400 MHz, $CDCl_3$): $\delta = 8.72$ (d, $J = 2.0$ Hz, 1H, pyridine-H), 8.62 (d, $J = 1.6$ Hz, 1H, pyridine-H), 7.87 (t, $J = 2.0$ Hz, 1H, pyridine-H), 7.86 (s, 1H, thienyl-H), 7.43 (d, $J = 3.6$ Hz, 2H, Ar-H), 7.28–7.26 (m, 1H, Ar-H), 7.15 (d, $J = 7.6$ Hz, 1H, Ar-H), 2.92–2.85 (m, 1H, CH), 1.17 (d, $J = 6.8$ Hz, 6H, $2CH_3$) . ESI-MS: m/z = 380.8$[M + H]^+$.

5-((5-(2-isopropylphenyl)pyridin-3-yl)thio)thiophene-2-carboxylic acid (24) ^{1}H NMR (400 MHz, $CDCl_3$): $\delta = 7.54$ (s, 1H, pyridine-H), 7.38 (s, 2H, pyridine-H), 7.19–7.16 (m, 2H, thienyl-H), 7.06–7.01 (m, 2H, Ar-H), 6.90 (d, $J = 8.8$ Hz, 2H, Ar-H), 2.67–2.56 (m, 1H, CH), and 0.90 (d, $J = 6.6$ Hz, 6H, $2CH_3$). ESI-MS: m/z = 356.1$[M + H]^+$.

General procedure for the synthesis of compounds 25–30

To a solution of compounds **19–24** (1.0 mmol, 1.0 eq) and DMF (7.6 mg, 103.5 μmol, 8.0 uL, 0.1 eq) in CH_2Cl_2 (10.0 mL), and $(COCl)_2$ (131.4 mg, 1.0 mmol, 91.0 μL, 1.0 eq) was added. The reaction was stirred at 25 °C for 1 h. The reaction was concentrated in vacuo to give the compounds **25–30**, which was put into next step without further purification.

General procedure for the synthesis of target compounds 31–50

A solution of compounds **25–30** (600.0 μmol, 1.0 eq), corresponding amine (660.0 μmol, 1.1 eq), and Et_3N (121.4 mg, 1.2 mmol, 166.0 μL, 2.0 eq) in CH_2Cl_2 (5.0 mL) was stirred at 25 °C for 16 h. The reaction was concentrated in vacuo. The residue was purified by prep-HPLC (0.1% HCl as additive) to give the target compounds **31–50**.

2-((5-(2-isopropylphenyl)pyridin-3-yl)thio)-*N*-phenylthiazole-5-carboxamide (31) White solid; Yield: 71.8%; Purity: 95.7%. ^{1}H NMR (400 MHz, $CDCl_3$): $\delta = 8.79$ (s, 1H, pyridine-H), 8.56 (s, 1H, pyridine-H), 8.15 (s, 1H, pyridine-H), 8.00–7.95 (m, 2H, thiazole-H, NH), 7.53 (d, $J = 8.0$ Hz, 2H, Ar-H), 7.38 (d, $J = 4.0$ Hz, 2H, Ar-H), 7.28 (t, $J = 7.6$ Hz, 2H, Ar-H), 7.24–7.20 (m, 1H, Ar-H), 7.11–7.07 (m, 2H, Ar-H), 2.88–2.81 (m, 1H, CH), and 1.12 (d, $J = 6.8$ Hz, 6H, $2CH_3$). ^{13}C NMR (100 MHz, d_6-DMSO): $\delta = 170.07$, 158.27, 152.12, 151.01, 146.69, 144.95, 142.90, 138.80, 138.70, 137.00, 135.80, 130.31, 129.51, 129.20, 127.60, 126.35, 126.31, 124.60, 120.89, 29.66, and 24.31. ESI-MS: m/z = 431.8$[M + H]^+$.

***N*-(4-fluorophenyl)-2-((5-(2-isopropylphenyl)pyridin-3-yl)thio)thiazole-5-carboxamide (32)** White solid; Yield: 35.7%; Purity: 95.1%. ^{1}H NMR (400 MHz, d_6-DMSO): $\delta = 10.49$ (s, 1H, NH), 8.90 (d, $J = 2.0$ Hz, 1H, pyridine-H), 8.70 (d, $J = 2.0$ Hz, 1H, pyridine-H), 8.53 (s, 1H, pyridine-H), 8.18 (t, $J = 2.0$ Hz, 1H, thiazole-H), 7.70–7.66 (m, 2H, Ar-H), 7.50–7.42 (m, 2H, Ar-H), 7.30 (td, $J = 7.6$, 1.2 Hz, 1H, Ar-H), 7.25–7.17 (m, 3H, Ar-H), 2.95–2.88 (m, 1H, CH), and 1.13 (d, $J = 6.8$ Hz, 6H, $2CH_3$). ^{13}C NMR (100 MHz, d_6-DMSO): $\delta = 170.34$, 160.20, 158.23, 157.81, 152.44, 151.32, 146.68, 144.99, 142.67, 138.72, 136.69, 135.88, 135.05, 135.03, 130.30, 129.48, 127.40, 126.34, 126.29, 122.82, 122.74, 115.94, 115.72, 29.66, and 24.31. ESI-MS: m/z = 449.9$[M + H]^+$.

2-((5-(2-isopropylphenyl)pyridin-3-yl)thio)-*N*-(4-methoxyphenyl)thiazole-5-carboxamide (33) Yellow solid; Yield: 61.4%; Purity: 99.5%. ^{1}H NMR (400 MHz, MeOD): $\delta = 8.86$ (d, $J = 2.0$ Hz, 1H, pyridine-H), 8.64 (d, $J = 1.2$ Hz, 1H, pyridine-H), 8.35 (s, 1H, pyridine-H), 8.15 (t, $J = 2.0$ Hz, 1H, thiazole-H), 7.53–7.42 (m, 4H, Ar-H), 7.30 (td, $J = 7.6$, 1.6 Hz, 1H, Ar-H), 7.23 (dd, $J = 7.6$, 1.2 Hz, 1H, Ar-H), 6.93–6.89 (m, 2H, Ar-H), 3.79 (s, 3H, CH_3), 2.99–2.95 (m, 1H, CH), and 1.20 (d, $J = 6.8$ Hz, 6H, $2CH_3$). ^{13}C NMR (100 MHz, d_6-DMSO): $\delta = 169.80$, 157.90, 156.37, 152.38, 151.26, 146.69, 144.59, 142.59, 138.70, 137.14, 135.89, 131.65, 130.30, 129.47, 127.49, 126.34, 126.30, 122.54, 114.37, 55.67, 29.66, and 24.31. ESI-MS: m/z = 462.0$[M + H]^+$.

***N*-benzyl-2-((5-(2-isopropylphenyl)pyridin-3-yl)thio)thiazole-5-carboxamide (34)** White solid; Yield: 64.9%; Purity: 99.8%. ^{1}H NMR (400 MHz, $CDCl_3$): $\delta = 8.80$ (s, 1H, pyridine-H), 8.61 (s, 1H, thiazole-H), 8.01 (d, $J = 6.8$ Hz, 2H, pyridine-H), 7.44 (d, $J = 4.0$ Hz, 2H, Ar-H), 7.36–7.26 (m, 6H, Ar-H), 7.16 (d, $J = 7.6$ Hz, 1H, Ar-H), 6.48 (s, 1H, NH), 4.57 (d, $J = 5.6$ Hz, 2H, CH_2), 2.94–2.88 (m, 1H, CH), and 1.17 (d, $J = 6.8$ Hz, 6H, $2CH_3$). ^{13}C NMR (100 MHz, d_6-DMSO): $\delta = 169.08$, 159.58, 152.13, 151.01, 146.69, 144.14, 142.65, 139.39, 138.70, 136.77, 135.84, 130.30, 129.48, 128.82, 127.77, 127.67, 127.42, 126.34, 126.30, 42.99, 29.63, and 24.30. ESI-MS: m/z = 445.9$[M + H]^+$.

2-((5-(2-isopropylphenyl)pyridin-3-yl)thio)-*N*-(1-methylpiperidin-4-yl)thiazole-5-carboxamide (35) White solid; Yield: 63.5%; Purity: 97.1%. ^{1}H NMR (400 MHz, $CDCl_3$): $\delta = 8.95$ (d, $J = 6.4$ Hz, 1H, pyridine-H), 8.62 (s, 1H, pyridine-H), 8.55 (s, 2H, Ar-H), 8.08 (s, 1H thiazole-H), 7.43 (d, $J = 4.0$ Hz, 2H, Ar-H), 7.28–7.24 (m, 1H, Ar-H), 7.17 (d, $J = 7.6$ Hz, 1H, NH), 4.23 (s, 3H, CH_2, CH), 3.59 (d, $J = 10.8$ Hz, 1H, CH_2), 3.08–2.98 (m, 2H, CH_2), 2.92–2.84 (m, 3H, CH_2, CH), 2.49–2.40 (m, 2H, CH_3), 2.18 (d, $J =$ 12.4 Hz, 2H, CH_2), and 1.17 (d, $J = 6.8$ Hz, 6H, $2CH_3$). ^{13}C NMR (100 MHz, d_6-DMSO): $\delta = 169.07$, 159.12, 151.97, 150.88, 146.68, 144.39, 142.72, 138.74, 136.73, 135.80, 130.29, 129.51, 127.77, 126.34, 126.31, 52.85, 49.31, 44.87, 42.83, 29.64, 29.03, 26.36, and 24.31. ESI-MS: $m/z = 453.0[M + H]^+$.

(2-((5-(2-isopropylphenyl)pyridin-3-yl)thio)thiazol-5-yl)(4-methylpiperazin-1-yl)methanone (36) White solid; Yield: 47.0%; Purity: 97.1%. ^{1}H NMR (400 MHz, $CDCl_3$): $\delta =$ 9.02 (s, 1H, pyridine-H), 8.65 (s, 1H, pyridine-H), 8.25 (s, 1H, pyridine-H), 8.04 (s, 1H, thiazole-H), 7.48–7.43 (m, 2H, Ar-H), 7.28–7.26 (m, 1H, Ar-H), 7.17 (d, $J = 7.2$ Hz, 1H, Ar-H), 5.86 (s, 2H, CH_2), 4.48 (s, 2H, CH_2), 3.59 (s, 2H, CH_2), 3.19 (s, 2H, CH_2), 2.93 (s, 3H, CH_3), 2.83 (t, $J =$ 6.8 Hz, 1H, CH), and 1.17 (d, $J = 6.4$ Hz, 6H, $2CH_3$). ^{13}C NMR (100 MHz, d_6-DMSO): $\delta = 168.41$, 160.29, 151.98, 150.84, 146.67, 144.85, 142.76, 138.75, 135.76, 133.36, 130.32, 129.54, 127.65, 126.37, 126.32, 52.31, 42.48, 29.66, and 24.31. ESI-MS: $m/z = 439.0[M + H]^+$.

2-((5-(2-ethylphenyl)pyridin-3-yl)thio)-*N*-(4-fluorophenyl) thiazole-5-carboxamide (37) White solid; Yield: 48.8%; Purity: 99.4%. ^{1}H NMR (400 MHz, MeOD): $\delta = 8.96$ (d, $J = 1.6$ Hz, 1H, pyridine-H), 8.75 (d, $J = 1.6$ Hz, 1H, thiazole-H), 8.39 (s, 1H, pyridine-H), 8.38 (t, $J = 2.0$ Hz, 1H, pyridine-H), 7.67–7.62 (m, 2H, Ar-H), 7.46–7.41 (m, 2H, Ar-H), 7.36–7.31 (m, 1H, Ar-H), 7.28 (d, $J = 7.6$ Hz, 1H, Ar-H), 7.13–7.07 (m, 2H, Ar-H), 2.65 (q, $J = 7.6$, 15.2 Hz, 2H, CH_2), and 1.12 (t, $J = 7.6$ Hz, 3H, CH_3). ^{13}C NMR (100 MHz, d_6-DMSO): $\delta = 170.12$, 160.20, 158.24, 157.80, 152.15, 152.07, 150.92, 150.84, 145.04, 143.04, 142.98, 141.97, 138.74, 136.79, 136.76, 136.29, 136.27, 135.06, 130.44, 129.40, 129.34, 127.60, 126.63, 122.81, 122.73, 115.91, 115.69, 26.00, and 15.79. ESI-MS: $m/z = 435.9[M + H]^+$.

***N*-benzyl-2-((5-(2-ethylphenyl)pyridin-3-yl)thio)thiazole-5-carboxamide (38)** White solid; Yield: 15.1%; Purity: 99.8%. ^{1}H NMR (400 MHz, MeOD): $\delta = 8.99$ (d, $J =$ 2.0 Hz, 1H, pyridine-H), 8.78 (d, $J = 2.0$ Hz, 1H, pyridine-H), 8.47 (t, $J = 2.0$ Hz, 1H, pyridine-H), 8.25 (s, 1H, thiazole-H), 7.48–7.42 (m, 2H, Ar-H), 7.37–7.33 (m, 5H, Ar-H), 7.30–7.24 (m, 2H, Ar-H), 4.52 (s, 2H, CH_2), 2.63 (q, $J = 7.6$, 15.2 Hz, 2H, CH_2), and 1.11 (t, $J = 7.6$ Hz, 3H, CH_3). ^{13}C NMR (100 MHz, d_6-DMSO): $\delta = 170.08$, 160.20, 158.28, 157.80, 156.73, 151.41, 150.83, 145.15, 143.37, 136.70, 135.72, 135.08, 135.06, 131.04, 130.95, 127.50, 124.94, 122.83, 122.76, 121.57, 115.91, 115.69, 112.44, and 56.17. ESI-MS: $m/z = 437.9[M + H]^+$.

***N*-(4-fluorophenyl)-2-((5-(2-methoxyphenyl)pyridin-3-yl) thio)thiazole-5-carboxamide (39)** White solid; Yield: 24.9%; Purity: 99.7%. ^{1}H NMR (400 MHz, MeOD): $\delta =$ 9.03 (d, $J = 6.4$ Hz, 2H, pyridine-H), 8.83 (s, 1H, pyridine-H), 8.44 (s, 1H, thiazole-H), 7.68–7.64 (m, 2H, pyridine-H), 7.55–7.51 (m, 2H, Ar-H), 7.23–7.09 (m, 4H, Ar-H), and 3.91 (s, 3H, CH_3). ^{13}C NMR (100 MHz, d_6-DMSO) : $\delta =$ 169.12, 159.59, 152.12, 150.86, 144.19, 142.78, 141.95, 139.40, 138.67, 136.75, 136.33, 130.44, 129.39, 129.32, 128.81, 127.78, 127.72, 127.42, 126.62, 43.00, 25.98, and 15.78. ESI-MS: $m/z = 432.0[M + H]^+$.

***N*-benzyl-2-((5-(2-methoxyphenyl)pyridin-3-yl)thio)thiazole-5-carboxamide (40)** White solid; Yield: 36.9%; Purity: 98.8%. ^{1}H NMR (400 MHz, MeOD): $\delta = 8.99$ (d, $J =$ 2.0 Hz, 1H, pyridine-H), 8.96 (d, $J = 2.0$ Hz, 1H, pyridine-H), 8.75 (t, $J = 2.0$ Hz, 1H, pyridine-H), 8.27 (s, 1H, thiazole-H), 7.54–7.48 (m, 2H, Ar-H), 7.33 (d, $J = 4.4$ Hz, 4H, Ar-H), 7.29–7.24 (m, 1H, Ar-H), 7.21–7.13 (m, 2H, Ar-H), 4.52 (s, 2H, CH_2), and 3.87 (s, 3H, CH_3). ^{13}C NMR (100 MHz, d_6-DMSO): $\delta = 169.01$, 159.61, 156.72, 151.34, 150.73, 144.27, 143.21, 139.40, 136.71, 135.66, 131.02, 130.95, 128.81, 127.79, 127.64, 127.41, 124.95, 121.57, 112.44, 56.15, and 43.00. ESI-MS: $m/z = 433.9[M + H]^+$.

***N*-(4-fluorophenyl)-5-((5-(2-isopropylphenyl)pyridin-3-yl) thio)-4-nitrothiophene-2-carboxamide (41)** White solid; Yield: 30.4%; Purity: 99.6%. ^{1}H NMR (400 MHz, d_6-DMSO): $\delta = 10.59$ (s, 1H, thienyl-H), 8.94 (d, $J = 2.0$ Hz, 1H, pyridine-H), 8.77 (d, $J = 2.0$ Hz, 1H, pyridine-H), 8.70 (s, 1H, pyridine-H), 8.28 (t, $J = 2.0$ Hz, 1H, NH), 7.70–7.66 (m, 2H, Ar-H), 7.49–7.42 (m, 2H, Ar-H), 7.32–7.17 (m, 4H, Ar-H), 2.98–2.91 (m, 1H, CH), and 1.13 (d, $J = 6.4$ Hz, 6H, $2CH_3$). ^{13}C NMR (100 MHz, d_6-DMSO): $\delta = 155.73$, 155.05, 152.82, 151.93, 146.19, 143.20, 140.71, 138.50, 135.39, 134.41, 129.80, 129.00, 126.74, 125.87, 125.75, 124.57, 122.08, 122.00, 115.59, 115.36, 29.24, and 23.72. ESI-MS: $m/z = 493.9[M + H]^+$.

***N*-benzyl-5-((5-(2-isopropylphenyl)pyridin-3-yl)thio)-4-nitrothiophene-2-carboxamide (42)** White solid; Yield: 41.5%; Purity: 99.9%. ^{1}H NMR (400 MHz, $CDCl_3$): $\delta =$ 8.86 (s, 1H, pyridine-H), 8.75 (s, 1H, pyridine-H), 8.08 (s, 1H, pyridine-H), 7.94 (s, 1H, thienyl-H), 7.46 (d, $J =$ 4.0 Hz, 2H, Ar-H), 7.36–7.27 (m, 6H, Ar-H), 7.20 (d, $J =$ 7.6 Hz, 1H, Ar-H), 6.55 (s, 1H, NH), 4.56 (d, $J = 5.6$ Hz,

2H, CH_2), 2.97–2.90 (m, 1H, CH), and 1.20 (d, $J = 6.4$ Hz, 6H, $2CH_3$). ^{13}C NMR (100 MHz, d_6-DMSO): $\delta = 159.67$, 154.44, 153.20, 152.22, 146.74, 143.80, 141.25, 139.13, 139.04, 136.03, 135.80, 130.28, 129.54, 128.82, 127.87, 127.50, 127.38, 126.35, 126.26, 124.15, 43.14, 29.71, and 24.19. ESI-MS: m/z = 489.9$[M + H]^+$.

5-((5-(2-isopropylphenyl)pyridin-3-yl)thio)-*N*-(1-methylpiperidin-4-yl)-4-nitrothiophene-2-carboxamide (43) White solid; Yield: 53.1%; Purity: 99.6%. ^{1}H NMR (400 MHz, MeOD): $\delta = 9.10$ (d, $J = 2.0$ Hz, 1H, pyridine-H), 8.90 (d, $J = 2.0$ Hz, 1H, pyridine-H), 8.56 (t, $J = 2.0$ Hz, 1H, pyridine-H), 8.35 (s, 1H, thienyl-H), 7.54–7.48 (m, 2H, Ar-H), 7.36–7.29 (m, 2H, Ar-H), 3.59 (d, $J = 12.8$ Hz, 2H, CH_2), 3.16 (t, $J = 12.4$ Hz, 2H, 2CH), 3.02–2.94 (m, 2H, CH_2), 2.89 (s, 3H, CH_3), 2.21 (d, $J = 13.6$ Hz, 2H, CH_2), 1.98–1.88 (m, 2H, CH_2), and 1.22 (d, $J = 6.8$ Hz, 6H, $2CH_3$). ^{13}C NMR (100 MHz, d_6-DMSO) : $\delta = 159.78$, 159.17, 154.31, 152.96, 151.99, 146.73, 143.99, 141.26, 141.19, 139.08, 135.94, 135.71, 130.25, 129.58, 127.49, 126.35, 126.26, 124.42, 52.75, 44.91, 42.79, 29.71, 28.94, and 24.19. ESI-MS: m/z = 497.0$[M + H]^+$.

(5-((5-(2-isopropylphenyl)pyridin-3-yl)thio)-4-nitrothiophen-2-yl)(4-methylpiperazin-1-yl) methanone (44) White solid; Yield: 53.1%; Purity: 99.7%. ^{1}H NMR (400 MHz, MeOD): $\delta = 9.04$ (d, $J = 1.6$ Hz, 1H, pyridine-H), 8.84 (d, $J = 1.6$ Hz, 1H, pyridine-H), 8.45 (d, $J = 2.0$ Hz, 1H, pyridine-H), 8.04 (s, 1H, thienyl-H), 7.54–7.47 (m, 2H, Ar-H), 7.39(t, $J = 7.6$ Hz, 1H, Ar-H), 7.28 (d, $J = 7.6$ Hz, 1H, Ar-H), 4.56 (d, $J = 14.0$ Hz, 2H, CH_2), 3.61–6.52 (m, 4H, $2CH_2$), 3.20 (t, $J = 11.6$ Hz, 2H, CH_2), 3.00 (t, $J = 6.8$ Hz, 1H, CH), 2.96(s, 3H, CH_3), and 1.23 (d, $J = 6.8$ Hz, 6H, $2CH_3$). ^{13}C NMR (100 MHz, d_6-DMSO): $\delta = 160.73$, 153.98, 153.24, 152.24, 146.71, 143.80, 140.54, 139.05, 135.75, 133.29, 130.31, 129.58, 127.30, 126.37, 126.30, 125.57, 52.19, 42.47, 29.72, and 24.24. ESI-MS: m/z = 482.9$[M + H]^+$.

4-cyano-N-(4-fluorophenyl)-5-((5-(2-isopropylphenyl)pyridin-3-yl)thio)thiophene-2-carboxamide (45) White solid; Yield: 53.1%; Purity: 99.3%. ^{1}H NMR (400 MHz, MeOD) : $\delta = 8.87$ (d, $J = 1.6$ Hz, 1H, pyridine-H), 8.67 (d, $J = 1.6$ Hz, 1H, pyridine-H), 8.13 (s, 2H, pyridine-H, thienyl-H), 7.69–7.66 (m, 2H, Ar-H), 7.51–7.45 (m, 2H, Ar-H), 7.32 (dt, $J = 7.6$, 1.6 Hz, 1H, Ar-H), 7.24 (d, $J = 7.6$ Hz, 1H, Ar-H), 7.14–7.10 (m, 2H, Ar-H), 2.91–2.84 (m, 1H, CH), and 1.18 (d, $J = 6.8$ Hz, 6H, $2CH_3$). ^{13}C NMR (100 MHz, d_6-DMSO): $\delta = 157.55$, 149.83, 149.74, 146.15, 142.44, 139.43, 138.07, 135.39, 134.28, 130.80, 129.77, 129.43, 128.96, 125.86, 122.31, 122.23, 115.59, 115.37, 113.25, 112.60, 29.16, and 23.84. ESI-MS: m/z = 473.9$[M + H]^+$.

***N*-benzyl-4-cyano-5-((5-(2-isopropylphenyl)pyridin-3-yl)thio)thiophene-2-carboxamide (46)** White solid; Yield: 35.9%; Purity: 99.2%. ^{1}H NMR (400 MHz, MeOD) : $\delta = 8.84$ (d, $J = 2.0$ Hz, 1H, pyridine-H), 8.64 (d, $J = 2.0$ Hz, 1H, pyridine-H), 8.07 (t, $J = 2.0$ Hz, 1H, pyridine-H), 7.94 (s, 1H, thienyl-H), 7.50–7.45 (m, 2H, Ar-H), 7.35–7.22 (m, 7H, Ar-H), 4.54 (s, 2H, CH_2), 2.87–2.80 (m, 1H, CH), and 1.16 (t, $J = 6.8$ Hz, 6H, $2CH_3$). ^{13}C NMR (100 MHz, d_6-DMSO): $\delta = 159.45$, 149.68, 149.51, 149.41, 146.64, 143.61, 139.91, 139.15, 138.61, 135.76, 130.53, 130.42, 130.26, 129.49, 128.82, 127.84, 127.49, 126.32, 113.93, 113.82, 43.14, 29.61, and 24.29. ESI-MS: m/z = 470.0$[M + H]^+$.

4-cyano-5-((5-(2-isopropylphenyl)pyridin-3-yl)thio)-*N*-(1-methylpiperidin-4-yl)thiophene-2-carboxamide (47) White solid; Yield: 37.5%; Purity: 95.6%. ^{1}H NMR (400 MHz, MeOD): $\delta = 8.92$ (s, 1H, pyridine-H), 8.73 (s, 1H, pyridine-H), 8.22 (s, 1H, pyridine-H), 8.05–8.03 (m, 1H, thienyl-H), 7.53–7.47 (m, 2H, Ar-H), 7.35–7.24 (m, 2H, Ar-H), 4.14–4.08 (m, 1H, CH), 3.60 (d, $J = 13.2$ Hz, 2H, CH_2), 3.17 (t, $J = 13.2$ Hz, 2H, CH_2), 2.95–2.82 (m, 4H, CH_3, CH), 2.23 (d, $J = 14.0$ Hz, 2H, CH_2), 1.97 (t, $J = 14.0$ Hz, 2H, CH_2), and 1.17 (d, $J = 6.8$, Hz, 6H, $2CH_3$). ^{13}C NMR (100 MHz, d_6-DMSO): $\delta = 158.97$, 149.75, 149.58, 149.48, 146.63, 143.46, 139.82, 138.58, 135.78, 130.77, 130.47, 130.25, 129.49, 126.32, 113.79, 113.75, 52.79, 44.98, 42.82, 29.61, 28.95, and 24.29. ESI-MS: m/z = 477.0$[M + H]^+$.

2-((5-(2-isopropylphenyl)pyridin-3-yl)thio)-5-(4-methylpiperazine-1-carbonyl)thiophene-3-carbonitrile (48) Yellow solid; Yield: 37.5%; Purity: 97.5%. ^{1}H NMR (400 MHz, MeOD): $\delta = 9.00$ (d, $J = 2.0$ Hz, 1H, pyridine-H), 8.80 (d, $J = 1.6$ Hz, 1H, pyridine-H), 8.37 (t, $J = 2.0$ Hz, 1H, pyridine-H), 7.89 (s, 1H, thienyl-H), 7.55–7.49 (m, 2H, Ar-H), 7.37–7.27 (m, 2H, Ar-H), 4.54 (d, $J = 14.1$ Hz, 2H, CH_2), 3.61 (d, $J = 12.8$ Hz, 4H, $2CH_2$), 3.24 (t, $J = 14.6$ Hz, 2H, CH_2), 2.98(s, 3H, CH_3), 2.88–2.81 (m, 1H, CH), and 1.23 (d, $J = 6.8$ Hz, 6H, $2CH_3$). ^{13}C NMR (100 MHz, d_6-DMSO): $\delta = 160.54$, 149.44, 149.24, 148.54, 146.66, 140.42, 140.05, 138.66, 135.67, 132.12, 130.56, 130.29, 129.55, 126.34, 113.90, 113.57, 52.26, 42.44, 29.63, and 24.32. ESI-MS: m/z = 463.0$[M + H]^+$.

***N*-(4-fluorophenyl)-5-((5-(2-isopropylphenyl)pyridin-3-yl)thio)thiophene-2-carboxamide (49)** White solid; Yield: 12.6%; Purity: 99.6%. ^{1}H NMR (400 MHz, $CDCl_3$): $\delta = 8.38$ (s, 2H, thienyl-H), 8.27 (s, 1H, pyridine-H), 7.72 (s, 2H, pyridine-H), 7.61 (dd, $J = 8.8$, 4.8 Hz, 2H, Ar-H), 7.46–7.42 (m, 2H, Ar-H), 7.33 (s, 1H, Ar-H), 7.10 (d, $J = 7.6$ Hz, 1H, Ar-H), 7.03 (t, $J = 8.4$ Hz, 2H, Ar-H), 2.82–2.78 (m, 1H, CH), and 1.15 (d, $J = 6.8$ Hz, 6H, CH_3). ^{13}C NMR (100 MHz, d_6-DMSO): $\delta = 160.17$, 159.24,

157.78, 147.32, 146.59, 146.39, 145.19, 138.32, 137.41, 137.19, 135.82, 135.54, 135.22, 135.20, 134.24, 130.66, 130.23, 129.46, 126.37, 126.33, 122.91, 122.83, 115.88, 115.65, 29.58, and 24.35. ESI-MS: m/z = 448.9$[M + H]^+$.

***N*-benzyl-5-((5-(2-isopropylphenyl)pyridin-3-yl)thio)thiophene-2-carboxamide (50)** White solid; Yield: 15.6%; Purity: 99.6%. ^{1}H NMR (400 MHz, $CDCl_3$): $\delta = 8.38$ (s, 2H, pyridine-H), 7.71 (s, 1H, pyridine-H), 7.51 (s, 1H, Ar-H), 7.47–7.41 (m, 2H, thienyl-H), 7.35–7.26 (m, 7H, Ar-H), 7.10 (d, $J = 7.6$ Hz, 1H, Ar-H), 6.53 (s, 1H, NH), 4.61 (d, $J = 1.6$ Hz, 2H, CH_2), 2.80–2.73 (m, 1H, CH), and 1.13 (d, $J = 6.4$ Hz, 6H, $2CH_3$). ^{13}C NMR (100 MHz, d_6-DMSO): $\delta = 160.58$, 147.11, 146.59, 146.08, 145.56, 139.62, 138.29, 137.54, 137.20, 135.79, 134.20, 130.23, 129.59, 129.46, 128.78, 127.73, 127.36, 126.38, 126.33, 42.99, 29.54, and 24.35. ESI-MS: m/z = 445.0$[M + H]^+$.

Similarity search and molecular docking

The 3D shape similarity to the reference molecule compound III-**106** was calculated by using Phase (Schrödinger, LLC, New York, NY, 2018. All the software used for similarity search and docking study belong to the same company.). Each molecule was prepared by LigPrep to generate their 3D structure, and their conformers were generated by using ConfGen. Each conformer from a given molecule is aligned to the reference molecule, and a similarity is computed based on overlapping hard-sphere volumes. MacroModel types were chosen as atom typing in the shape similarity calculation.

The molecular docking procedure was performed by using Glide with the default option. The cocrystal structure of IGF-1R (PDB ID: 5FXS) was selected as the docking template. For the preparation of protein, the hydrogen atoms were added by using protein preparation Wizard module of Maestro, and the OPLS3 force field was employed. For the preparation of ligands, the 3D structures were generated and their energy minimization was performed by using LigPrep. Conformers were generated by using ConfGen. A 30 Å docking grid was generated using centroid of ligand in the 5FXS crystal structure. Then the ligand was removed and compound was placed during the molecular docking procedure. Types of interaction of the docked IGF-1R with ligand were analyzed and then the docking conformations were selected and saved based on calculated glide docking energy score.

Biological evaluation

IGF-1R kinase activity assay

Effects of the tested compound on the activities of IGF1R kinases were evaluated by electrophoretic mobility shift assay with ATP concentration at 75 μM. Briefly, the compound was prepared as 50× of the final desired concentration stocks in 100% DMSO and directly diluted at five different concentrations (10 nM, 50 nM, 0.25 μM, 1.25 μM, and 6.25 μM) into the assay. The substrate solution contains 3 μM Peptide FAM-P13 (5-FAM-KKSRGDYMTMQIG-CONH2), 75 μM ATP, 50 mM HEPES (pH 7.5), 0.0015% Brij-35, and 10 mM $MgCl_2$. The kinase buffer contains 4 nM IGF-1R, 50 mM HEPES (pH 7.5), 0.0015% Brij-35, and 2 mM DTT. The stop buffer contains 100 mM HEPES (pH 7.5), 0.015% Brij-35, and 0.2% Coating Reagent #3 and 50 mM EDTA. Transfer 10 μL of compound to a new 96-well plate as the intermediate plate, add 90 μL kinase buffer to each well. Transfer 5 μL of each well from the 96-well intermediate plate to a 384-well plate in duplicates. Then 10 μL kinases solution was added to the 384-well plate. And then 10 μL substrate solution was added to each well. The plate was then incubated at 28 °C for 60 min. After incubation, then 25 μL stop buffer was added to stop the reaction. A reaction that contained no active enzyme and without compound was used as the DMSO control, and the staurosporine for the positive control. Read the conversion data on Caliper EZ reader II, convert conversion values to inhibition values. The inhibition rate (%) was calculated using the following equation = (max-conversion)/(max − min) × 100, "max" stands for the DMSO control and "min" stands for the low control. Fit the data in XLFit excel add-in version 5.4.0.8 to obtain the IC_{50} values.

Cell proliferation assay

The antiproliferative activities in vitro of the compounds were measured by the standard CTG assay. K562 (*Leukemia*), Hep-G2 (*Human liver cancer*), HCT-116 (*Colon cancer*), WSU-DLCL2 (*Lymphoma*), and A549 (*Non-small cell lung cancer*) cell lines were cultured in EMEM supplement with 10% fetal bovine serum (FBS). Briefly, cells were plated at a plating density of 4×10^3 cells per well, and incubated in 5% CO_2 at 37 °C for 24 h. The cells were treated with all the tested compounds at the indicated final concentrations, respectively (DMSO as the negative, and Paclitaxel as the positive), and then the cell cultures were continued to incubate for 72 h. Cell titer-Glo reagent was added to each well, and shake the plates for 10 min to induce cell lysis. Allow the plate incubates at room temperature for 2 min to stabilize luminescent signal, then the luminescence was read with Envision. The IC_{50} values were obtained by using the GraphPad Prism 5.0. All the target compounds were tested in each of cell lines, and the inhibition rates of proliferation were calculated with the following equation: Inhibition (%) = (Max signal − Compound signal)/(Max signal − Min signal) × 100. Max signal was obtained from the action of DMSO. Min signal was obtained from the action of medium only.

Enzymatic inhibitory assay

Method (*A*): For most assays, kinase-tagged T7 phage strains were grown in parallel in 24-well blocks in an *E. coli* host derived from the BL21 strain. *E. coli* were grown to log phase and infected with T7 phage from a frozen stock (multiplicity of infection = 0.4) and incubated with shaking at 32 °C until lysis (90–150 min). The lysates were centrifuged (6000 × *g*) and filtered (0.2 μm) to remove cell debris. The remaining kinases were produced in HEK-293 cells and subsequently tagged with DNA for qPCR detection. Streptavidin-coated magnetic beads were treated with biotinylated small molecule ligands for 30 min at room temperature to generate affinity resins for kinase assays. The liganded beads were blocked with excess biotin and washed with blocking buffer (SeaBlock (Pierce), 1% BSA, and 0.05% Tween 20, 1 mM DTT) to remove unbound ligand and to reduce nonspecific phage binding. Binding reactions were assembled by combining kinases, liganded affinity beads, and the tested compound in 1× binding buffer (20% SeaBlock, 0.17× PBS, 0.05% Tween 20, and 6 mM DTT). The tested compound was prepared as 40× stocks in 100% DMSO and directly diluted into the assay. All reactions were performed in polypropylene 384-well plates in a final volume of 20 μL. The assay plates were incubated at room temperature with shaking for 1 h and the affinity beads were washed with wash buffer (1× PBS, 0.05% Tween 20). The beads were then resuspended in elution buffer (1× PBS, 0.05% Tween 20, and 0.5 μM nonbiotinylated affinity ligand) and incubated at room temperature with shaking for 30 min. The kinase concentration in the eluates was measured by qPCR. The results for primary screen binding interactions are reported as "% Ctrl", which were calculated with the following equation: "% Ctrl" = (compound signal − positive control signal)/(negative control signal − positive control signal) × 100. Negative control as the DMSO control (100% Ctrl) and positive control stands for the control compound (0% Ctrl).

Method (*B*): Further evaluation of the enzymatic selectivity of the compounds against six kinases (AURA, JAK3, FGFR2, FGFR3, EGFR, and RON) with ATP concentration at *Km* was carried out by mobility shift assay. Dilute the tested compounds to 50× of the final desired highest inhibitor concentration in reaction by 100% DMSO. Then 5 μL of the tested compound solution was added to a 384-well plate. And then 10 μL kinases solution (4 nM kinases, 50 mM HEPES [pH 7.5], 0.0015% Brij-35, and 2 mM DTT) was added to the 384-well plate. Then 10 μL substrate solution (3 μM Peptide FAM-P13(5-FAM-KKSRGDYMTMQIG-CONH2), 75 μM ATP, 50 mM HEPES [pH 7.5], 0.0015% Brij-35, and 10 mM $MgCl_2$) was added to each well. The plate was then incubated at 28 °C for 60 min. After incubation, then 25 μL stop buffer (100 mM HEPES [pH 7.5], 0.015% Brij-35, 0.2% Coating Reagent #3, and 50 mM EDTA) was added to stop the reaction. A reaction that contained no active enzyme and without compound was used as the DMSO control, and the staurosporine for the positive control. Read the conversion data on Caliper EZ reader II, convert conversion values to inhibition values. The inhibition rate (%) was calculated using the following equation = (max-conversion)/(max − min) × 100, "max" stands for the DMSO control and "min" stands for the low control. Fit the data in XLFit excel add-in version 5.4.0.8 to obtain the IC_{50} values.

Flow cytometry analysis for cell cycle assay

Cell cycle arrest of Hep-G2 cells induced by the tested compound was measured by FACS. Hep-G2 cells at a density of 1×10^6 cells were treated with the tested compound (0.5, 1, 5, and 10 μM), Doxorubicin (0.5 μM, 1 μM) or DMSO (control) for 24 h. The cells were harvested by digestion with Trypsin-EDTA and centrifugation at 1500 rpm for 15 min. Fix the cells with 75% EtOH, and vortex the tube at half speed while adding EtOH to prevent clustering of cells during the fixation. Incubate on ice for 15 min and then stored at −20 °C overnight. Afterwards, PBS was added and centrifugation at 1500 rpm for 5 min, discard the supernatant. Then the cells were washed once by PBS (including 1%FBS), and incubated with PI/RNase Staining Buffer at room temperature for 20 min in the dark. Cells were analyzed by CytoFLEX at the lowest speed and results were analyzed by ModFit software.

Conclusions

In conclusion, a series of 3-(thiophen/thiazole-2-ylthio)pyridine derivatives were synthesized and evaluated. Different from what was envisaged, all the target compounds exhibited no inhibitory activities against IGF-1R. However, most analogues showed moderate to potent anticancer activities against various cancer cell lines. Representative compound **43** was further screened against more than 50 kinases, and potent activities were observed against kinases such as FGFR 3, FGFR 2, EGFR, JAK, and RON. Moreover, according to cell cycle assay, compound **43** induced G1/G0 phase arrest of the cell cycle in Hep-G2 cells. In the light of this study, 3-(thiophen/thiazole-2-ylthio)pyridine derivatives were considered to be multi-target anticancer agents, which are worth for further optimization for cancer treatment.

Acknowledgements The authors thank the project supported by the key Development Program of the Hangzhou Science and Technology Committee (Grant No. 20152013A03), the Research project on application of public welfare technology supported by Science Technology Department of Zhejiang Province (Grant No. 2017C33233 and LGF18H300001).

Compliance with ethical standards

Conflict of interest The authors declare that they have no conflict of interest.

Publisher's note: Springer Nature remains neutral with regard to jurisdictional claims in published maps and institutional affiliations.

References

Brahmkhatri VP, Prasanna C, Atreya HS (2015) Insulin-like growth factor system in cancer: novel targeted therapies. Biomed Res Int 2015:538019

Buchanan JL, Newcomb JR, Carney DP, Chaffee SC, Chai L, Cupples R, Epstein LF, Gallant P, Gu Y, Harmange JC, Hodge K, Houk BE, Huang X, Jona J, Joseph S, Jun HT, Kumar R, Li C, Lu J, Menges T, Morrison MJ, Novak PM, van der Plas S, Radinsky R, Rose PE, Sawant S, Sun JR, Surapaneni S, Turci SM, Xu K, Yanez E, Zhao H, Zhu X (2011) Discovery of 2, 4-bis-arylamino-1, 3-pyrimidines as insulin-like growth factor-1 receptor (IGF-1R) inhibitors. Bioorg Med Chem Lett 21:2394–2399

Carboni JM, Wittman M, Yang Z, Lee F, Greer A, Hurlburt W, Hillerman S, Cao C, Cantor GH, Dell-John J, Chen C, Discenza L, Menard K, Li A, Trainor G, Vyas D, Kramer R, Attar RM, Gottardis MM (2009) BMS-754807, a small molecule inhibitor of insulin-like growth factor-1R/IR. Mol Cancer Ther 8:3341–3349

Deng XQ, Xiang ML, Jia R, Yang SY (2007) Progress in the design of selective ATP-competitive inhibitors. Acta Pharm Sin 42:1232–1236

Furstenberger G, Senn HJ (2002) Insulin-like growth factors and cancer. Lancet Oncol 3:298–302

Kawauchi K, Ogasawara T, Yasuyama M, Otsuka K, Yamada O (2009) Regulation and importance of the PI3K/Akt/mTOR signaling pathway in hematologic malignancies. Anticancer Agents Med Chem 9:1024–1038

Girnita A, Girnita L, del Prete F, Bartolazzi A, Larsson O, Axelson M (2004) Cyclolignans as inhibitors of the insulin-like growth factor-1 receptor and malignant cell growth. Cancer Res 64:236–242

Gualberto A, Pollak M (2009) Clinical development of inhibitors of the insulin-like growth factor receptor in oncology. Curr Drug Targets 10:923–936

Hewish M, Chau I, Cunningham D (2009) Insulin-like growth factor 1 receptor targeted therapeutics: novel compounds and novel treatment strategies for cancer medicine. Recent Pat Anticancer Drug Discov 4:54–72

LeRoith D, Werner H, Beitner-Johnson D, Roberts Jr. CT (1995) Molecular and cellular aspects of the insulin-like growth factor I receptor. Endocr Rev 16:143–163

Mulvihill MJ, Cooke A, Rosenfeld-Franklin M, Buck E, Foreman K, Landfair D, O'Connor M, Pirritt C, Sun Y, Yao Y, Arnold LD, Gibson NW, Ji QS (2009) Discovery of OSI-906: a selective and orally efficacious dual inhibitor of the IGF-1 receptor and insulin receptor. Future Med Chem 1:1153–1171

Pollak M, Beamer W, Zhang JC (1998) Insulin-like growth factors and prostate cancer. Cancer Metastasis Rev 17:383–390

Rodon J, DeSantos V, Ferry Jr RJ, Kurzrock R (2008) Early drug development of inhibitors of the insulin-like growth factor-I receptor pathway: lessons from the first clinical trials. Mol Cancer Ther 7:2575–2588

Sachdev D, Yee D (2007) Disrupting insulin-like growth factor signaling as a potential cancer therapy. Mol Cancer Ther 6:1–12

Samani AA, Yakar S, LeRoith D, Brodt P (2007) The role of the IGF system in cancer growth and metastasis: overview and recent insights. Endocr Rev 28:20–47

Scagliotti GV, Novello S (2012) The role of the insulin-like growth factor signaling pathway in non-small cell lung cancer and other solid tumors. Cancer Treat Rev 38:292–302

Sepp-Lorenzino L (1998) Structure and function of the insulin-like growth factor I receptor. Breast Cancer Res Treat 47:235–253

Stewart CE, Rotwein P (1996) Growth, differentiation, and survival: multiple physiological functions for insulin-like growth factors. Physiol Rev 76:1005–1026

Sun WY, Yun HY, Song YJ, Kim H, Lee OJ, Nam SJ, Koo JS (2015) Insulin-like growth factor 1 receptor expression in breast cancer tissue and mammographic density. Mol Clin Oncol 3:572–580

Sun Y, Sun X, Shen B (2017) Molecular Imaging of IGF-1R in Cancer. Mol Imaging 16:1536012117736648

Treu, M (2010) New aminopyrazoloquinazolines. WO 2,012,010,704 (A1).

Trojan J, Cloix JF, Ardourel MY, Chatel M, Anthony DD (2007) Insulin-like growth factor type I biology and targeting in malignant gliomas. Neuroscience 145:795–811

Vanhaesebroeck B, Alessi DR (2000) The PI3K-PDK1 connection: more than just a road to PKB. Biochem J 346:561–576

Yeo CD, Park KH, Park CK, Lee SH, Kim SJ, Yoo HK, Lee YS, Lee EJ, Lee KY, Kim TJ (2015) Expression of insulin-like growth factor 1 receptor (IGF-1R) predicts poor responses to epidermal growth factor receptor (EGFR) tyrosine kinase inhibitors in non-small cell lung cancer patients harboring activating EGFR mutations. Lung cancer 87:311–317